ADVANCED HEALTHCARE MATERIALS
www.advhealthmat.de

Dual-Stage Crosslinking of a Gel-Phase Bioink Improves Cell Viability and Homogeneity for 3D Bioprinting

*Karen Dubbin, Yuki Hori, Kazuomori K. Lewis, and Sarah C. Heilshorn**

Tissue engineering strategies have been historically limited in their ability to precisely pattern multiple cell types to match the complexity of natural tissues. 3D printing has emerged as an ideal solution for this challenge, allowing engineers to design and construct multicellular architectures in minutes to hours.[1] While 3D printing of thermoplastics both in industry and the general public has seen vast growth in the past five years, translating this technology into cell-based printing is still an emerging field. A key limitation preventing the widespread use of cell-based additive patterning is the lack of cell-compatible bioinks that have the required properties for scalable 3D printing.[2] To date, most proof of concept bioprinting studies have utilized commercially available biomaterials or biomaterials that were previously reported in the literature and originally designed for other applications. As the community moves toward printing larger and more complex tissue constructs, more stringent requirements are demanded of the bioink. In particular, three current challenges of many commonly used bioinks prevent their use in scalable bioprinting technology; these include maintaining a homogeneous cell suspension in the print cartridge,[3] avoiding cell damage during extrusion,[4] and ensuring cellular hydration throughout the printing process.[5]

Hydrogels are a material of interest for tissue engineering applications, due to their ability to mimic cell interactions with the extracellular matrix.[6a-c] In many current bioprinting setups, the bioink is a viscous polymer solution into which cells are added in the print cartridge. Post-printing, the bioink is crosslinked to form a hydrogel that encapsulates the cells.[1] While use of viscous fluid bioinks facilitates easy loading into the print cartridge, it has three major drawbacks. First, cells in viscous fluids experience sedimentation,[7] resulting in printer clogging as well as inhomogeneous distributions in the print cartridge as well as in the final printed construct.[8,9] Second, cells in viscous fluids experience substantial shear and extensional forces during extrusion, resulting in cell membrane damage and death.[9,10] Third, viscous fluids are typically printed and crosslinked in air to avoid bioink dilution and flow, resulting in potential dehydration of the encapsulated cells. Each of these challenges are worsened by longer print times, which are required as the field advances to create more complex and larger printed structures.

To address the challenge of cell sedimentation in the print cartridge, suspensions of microgels or weak extrudable hydrogels have been used as bioinks.[11,12] However, most of these materials are still printed in air, which can lead to cell dehydration. Hydrogel bioinks also require higher print pressures, and it is unknown how these increased mechanical forces might impact cell viability during extrusion. To address these challenges, here we report the design and development of a new gel-phase bioink with dual-stage crosslinking that maintains cell homogeneity, provides mechanical protection during printing, and prints within an aqueous medium to prevent dehydration (**Figure 1**A).

The initial crosslinking mechanism is based on a two-component hydrogel with complementary peptide-binding domains designed into each component. This class of hydrogel is referred to as a mixing-induced two-component hydrogel, or MITCH.[13,14] Upon mixing, the complementary domains heteroassemble, forming physical crosslinks between the two components to create a weak hydrogel network (Figure 1B). Previously, our group has demonstrated that weak hydrogels can provide significant mechanical protection to encapsulated cells during clinically relevant cell transplantation procedures, as compared to cell transplantation using a fluid medium.[10,14,15] These weak hydrogels are thought to provide mechanical shielding during transport through the syringe needle, resulting in less cell membrane damage. Therefore, we hypothesized that a weak, physical hydrogel design may also be able to provide mechanical shielding during bioink printing. Furthermore, the presence of a gel-phase bioink within the print cartridge is expected to prevent cell sedimentation and printer clogging.[12] Upon application of low pressure, binding between the peptide-peptide domains should be disrupted, resulting in hydrogel shear-thinning into an easily extrudable bioink.

The first component of our new bioink is based on the polysaccharide Alginate, which is commonly used as a viscous fluid bioink.[1,16] To enable Alginate to function as a gel-phase bioink, we modified each Alginate chain (MW 75–200 kDa) with an average of about ten proline-rich peptide domains (termed P1) (Table S1 for amino acid sequence and Figure S1 of the Supporting Information) via NHS (*N*-hydroxysulfosuccinimide)-conjugation chemistry. The second component of the bioink is a recombinant, engineered protein (termed C7) developed by our group that contains seven repeats of a complementary

K. Dubbin, Dr. Y. Hori
Materials Science and Engineering
Stanford University
Stanford, CA 94305, USA
K. K. Lewis
Chemical Engineering
Stanford University
Stanford, CA 94305, USA
Prof. S. C. Heilshorn
Materials Science and Engineering, 476 Lomita Mall
Stanford University
Stanford, CA 94305, USA
E-mail: Heilshorn@stanford.edu

DOI: 10.1002/adhm.201600636

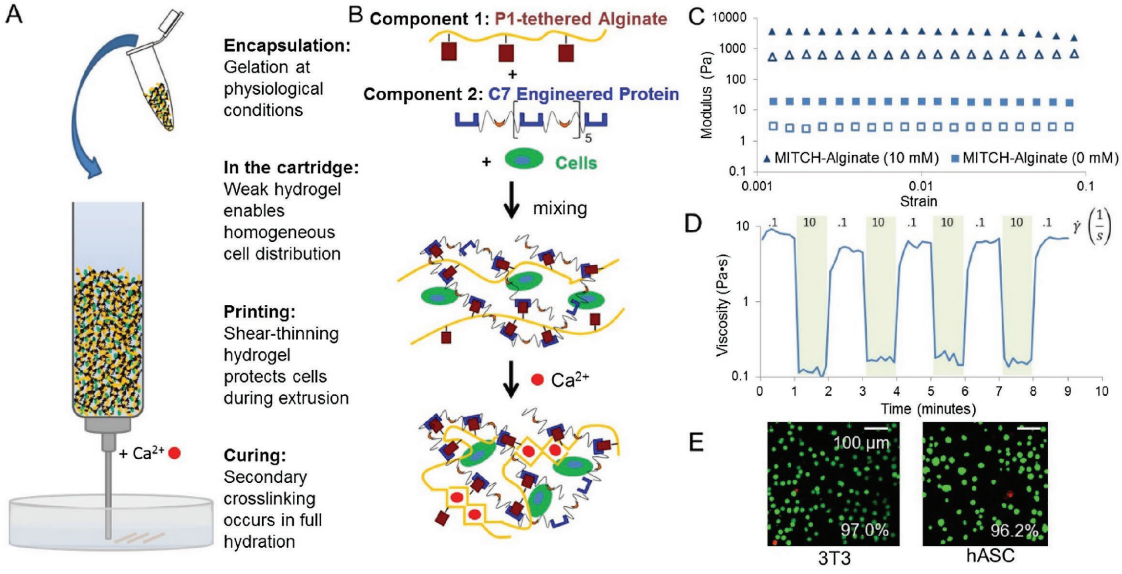

Figure 1. A) Schematic depicting the benefits of MITCH-Alginate bioink for each stage of the printing process. B) Schematic of the two material components of MITCH-Alginate and its dual-stage crosslinking. In the first stage, noncovalent binding between two complementary peptides forms a weak gel upon mixing of the two polymer components. In the second stage, ionic crosslinking occurs between calcium ions in solution and the alginate backbone of component 1. C) Storage moduli (G′, closed symbols) and loss moduli (G″, open symbols) of MITCH-Alginate after the first stage and second stage of crosslinking (0×10^{-3} and 10×10^{-3} M calcium, respectively), demonstrating a 100-fold increase in modulus after exposure to calcium. D) Rapid shear-thinning and self-healing behavior of MITCH-Alginate after the first stage of crosslinking mimics the material transition from within the cartridge (low shear, 0.1 s^{-1}) to passing through the nozzle (high shear, 10 s^{-1}). E) Live/Dead (green/red, respectively) staining of 3T3 fibroblast cells and hASCs encapsulated in MITCH-Alginate after the first stage of crosslinking confirms high cell viability (97.0% and 96.2%, respectively).

peptide that folds into a WW domain and heteroassembles with P1 in an exact 1:1 stoichiometry[13,17] (Table S1, Supporting Information). When mixed together, these two components form a new gel-phase bioink MITCH-Alginate. In the absence of divalent cations, MITCH-Alginate crosslinking occurs solely through the engineered peptide–peptide interactions, resulting in a weak hydrogel (G′ ≈ 20 Pa, Figure 1C). In contrast, when exposed to divalent cations (10×10^{-3} M calcium for 10 min), a secondary crosslinking step occurs along the Alginate backbone through ionic interactions,[18,19] stiffening the original hydrogel network over two orders of magnitude (G′ ≈ 4 kPa, 1C).[18]

Once exposed to calcium, the moduli and diffusivity properties of MITCH-Alginate are similar to unmodified Alginate (Figure S2, Supporting Information), but MITCH-Alginate provides the advantages of both a primary crosslinking step and the presence of cell-adhesive domains within the C7 protein. This dual-stage crosslinking strategy was hypothesized to enable direct printing into a fluid bath, as the MITCH-class of hydrogels formed through peptide–peptide interactions exhibit rapid self-healing (typically within seconds),[13–15,17] which should maintain the printed structure even upon extrusion within an aqueous solution. Printing directly into a calcium bath thus serves two roles: providing increased mechanical support to maintain the printed structure and preventing cell dehydration, which is a major cause of bioprinting cell death.[20] Scientists estimate that the therapeutic threshold for full organ replacement with a printed construct is between 1 and 10 billion viable cells per organ.[21] As tissue engineers begin to print these larger and more complex tissue constructs, the duration of printing time is estimated to be tens of hours.[22] Thus, for effective scale-up of 3D bioprinting technology, bioinks that enable printing within fully hydrated conditions will become even more critical. To confirm the rapid and reversible shear-thinning and self-healing of the primary crosslinking network within this new MITCH-Alginate formulation, alternating high and low shear rates (10 s^{-1} and 0.1 s^{-1}) were applied in the absence of calcium. When high shear rate was applied (as would be experienced in the nozzle during printing), viscosity decreased more than tenfold within 3 s. When low shear rate was applied (as would be experienced post-printing), viscosity rapidly increased for the first ≈3 s, indicative of return to the gel phase, followed by a gradual continued thickening for another ≈15 s until the maximal viscosity was achieved (Figure 1D). This shear-thinning and self-healing behavior was fully reversible across multiple cycles.

We next quantified cell viability after encapsulation in the newly developed hydrogel to evaluate cytocompatibility. Both fibroblasts (NIH 3T3s) and pluripotent stem cells (human adipose-derived stem cells, hASCs) were used as proof of concept cell types for this paper. Fibroblasts were selected for their role as a support cell and their influence in epithelial–mesenchymal interactions, which may be beneficial in printing multicell-type structures.[23] hASCs were selected due to their high potential for clinical translation, as they can be obtained using a relatively noninvasive isolation process from adult fat tissue lipoaspirate and provide excellent, patient-specific, regenerative potential.[24] Both fibroblasts and ASCs are components of adipose tissue, and combinations of stem cells and fibroblasts have been used for adipose tissue engineering.[25] Both 3T3s and hASCs exhibited high viability (97% and 96%, respectively) when encapsulated in MITCH-Alginate (0×10^{-3} M calcium) for 1 h and assessed using Live/Dead staining (Figure 1E). These data

Adv. Healthcare Mater. 2016,
DOI: 10.1002/adhm.201600636

support the hypothesis that encapsulation in a weak hydrogel formed through peptide–peptide interactions in the absence of chemical crosslinkers and initiators can maintain high levels of cell survival.

We next evaluated the ability of the MITCH-Alginate hydrogel to prevent cell sedimentation, which is a major bioprinting concern as print times become longer. Prelabeled 3T3s were homogenously dispersed in MITCH-Alginate or an unmodified Alginate solution as a control, both with 0×10^{-3} M calcium, and allowed to rest for 1 h. Imaging was performed along the z-axis of the cartridge, and the fraction of total cells in each quadrant along the z-axis was quantified. The cell fraction was similar (≈25%) across each quadrant for cells encapsulated in MITCH-Alginate, demonstrating that a homogenous cell dispersion was maintained. In contrast, for the Alginate solution, there were statistically fewer cells in quadrant 1 (i.e., the top quadrant) and statistically more cells in quadrant 4 (i.e., the bottom quadrant), demonstrating that significant cell sedimentation occurred in these samples (**Figure 2**A,B). Thus, these data confirm our hypothesis that a weak hydrogel is preferable to that of a viscous fluid for maintaining cell homogeneity within the print cartridge, even for relatively short print times of 1 h.

We next explored the potential cell-protective qualities of the new hydrogel during printing. To investigate this concept, cells were encapsulated in MITCH-Alginate and printed (cartridge = 10 mL syringe, nozzle = 32 gauge syringe, pressure = 10 psi) to determine the effect of extrusion through the nozzle on cell membrane integrity. For both cell types tested, 3T3s and hASCs, significantly fewer cells had damaged cell membranes (4% and 5%, respectively) when printed in MITCH-Alginate compared to unmodified Alginate (39% and 19%, respectively, Figure 2C,D). These data are consistent with the hypothesis that weak, gel-phase bioinks can significantly improve cell viability during extrusion printing, when compared to a viscous fluid bioink.

One of the main benefits of 3D printing is the ability to culture multiple cell types in geometrically patterned orientations. To evaluate the use of MITCH-Alginate in preparing patterned cell cocultures, we first evaluated the viability of each cell type individually for up to 7 d post-printing. At all time-points, both 3T3s and hASCs were greater than 90% viable, as quantified using Live/Dead imaging (**Figure 3**A). To demonstrate coculture patterning, 3T3s and hASCs were prelabeled with green and red fluorescent cell trackers, respectively. The first geometric pattern printed was a series of parallel lines alternating between 3T3s and hASCs (Figure 3B). After 7 d of culture post-printing, the geometric pattern was still evident with minimal cell migration across the stripe boundaries, demonstrating maintenance of the printed cell/bioink construct over time. As a second demonstration, 3T3s and hASCs were patterned into overlapping perpendicular lines (Figure 3C,D). After 7 d

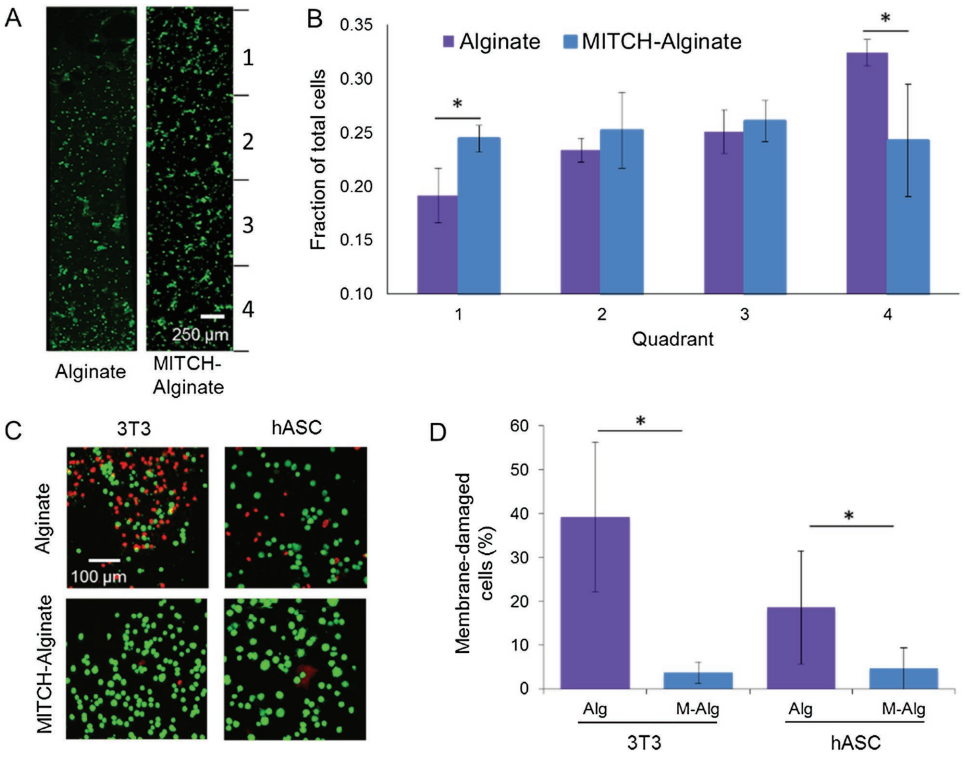

Figure 2. A) Representative images of prelabeled 3T3 cells after 1 h of encapsulation in unmodified Alginate or MITCH-Alginate; images were segmented into four vertical quadrants (each with a height of 875 μm) for quantification of cell density. B) Statistical analysis of cell density within each quadrant demonstrates significant cell sedimentation within Alginate, while MITCH-Alginate maintains a homogeneous cell suspension. C) Live/Dead (green/red, respectively) staining of cells immediately after printing with unmodified Alginate or MITCH-Alginate. D) Quantification of the percentage cells with membrane damage immediately after printing with Alginate (Alg) or MITCH-Alginate (M-Alg), demonstrating that MITCH-Alginate provides significant protection from mechanical damage during printing for both 3T3 cells and hASCs.

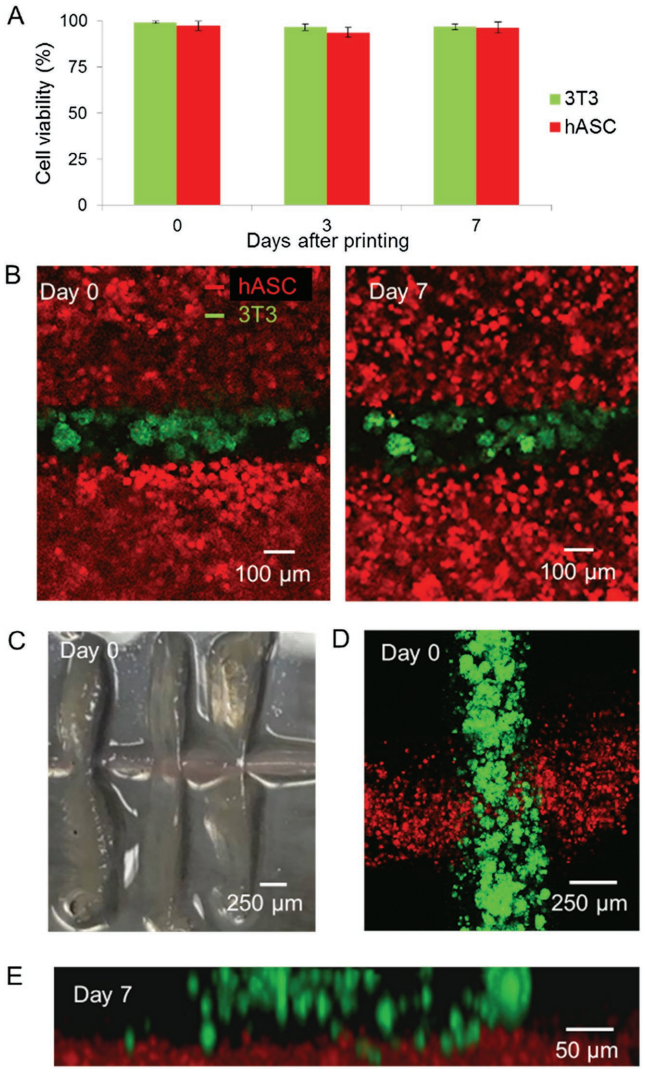

Figure 3. A) Quantified viability of 3T3 fibroblast cells and hASCs printed with MITCH-Alginate over 7 d post-printing. B) Spatial arrangement of prelabeled hASCs (red) and 3T3 cells (green) printed with MITCH-Alginate into a pattern of parallel lines at days 0 and 7, demonstrating long-term pattern maintenance. C) Macroscopic photograph and D) confocal microscopy image of prelabeled hASCs (red) and 3T3 cells (green) printed with MITCH-Alginate into a pattern of perpendicular lines (top-down view). E) Confocal microscopy z-stack of perpendicularly patterned 3T3 cells and hASCs at day 7, demonstrating cell layers retain their spatial fidelity over time.

of culture post-printing, fluorescent imaging at the cross-over sites revealed that the pattern maintained two distinct vertical cell layers, again with minimal cell migration between the two stripes (Figure 3E).

In conclusion, we present a novel, two-component bioink to address three critical needs in cell-based bioprinting: maintaining a homogeneous cell suspension in the print cartridge, avoiding cell membrane damage during extrusion, and ensuring cellular hydration throughout the printing process. These challenges were met by designing a shear-thinning hydrogel with two distinct crosslinking steps. In step one, molecular recognition between two complementary peptide domains results in a weak hydrogel that prevents cell sedimentation and provides significant mechanical protection from membrane damage during printing, and rapidly self-heals after extrusion into an aqueous bath. In step two, ionic crosslinking increases the storage modulus of the gel more than 100-fold, providing mechanical support post-printing and maintaining long-term print fidelity. This novel bioink enabled the patterning of highly viable cocultures that maintained their spatial organization over one week of culture. By addressing the limitations of many current bioinks, this two-stage bioink design strategy enables the scale-up of bioprinting technology to fabricate larger structures with more complex multicell patterns without compromising cell homogeneity or cell viability.

Experimental Section

Material Synthesis: P1 peptide (EYPPYPPPPYPSGC, 1536 g mol^{-1}) was purchased from Genscript Corp (Piscataway, NJ, USA) and Alginate was purchased from Novamatrix (Sandvika, Norway) in the LVG formulation (MW 75–200 kDa). Alginate (0.02 g mL^{-1}) was mixed with an equal volume of 0.2 M MES (2-(4-morpholino)ethanesulfonic acid sodium salt) buffer with 0.6 M NaCl, followed by addition of 5.2×10^{-3} M EDC (1-ethy/-3-[2-dimethylaminopropyl]carbodiimide hydrochloride) and 2.6×10^{-3} M sulfo-NHS, reaction scheme provided in Figure S3 of the Supporting Information. Within 5 min of the EDC and sulfo-NHS addition, 2 mg of P1 peptide per 10 mg of Alginate was mixed to the reaction solution. The solution was shaken for 20–24 h at room temperature and then dialyzed (7–10 kDa MWCO) against 4 L water for 2–3 d with 3–4 changes of the dialysis bath. The dialyzed solution was lyophilized, weighed, and reconstituted in water at a concentration of 0.01–0.02 g mL^{-1} immediately before use. To quantify the amount of P1 conjugated on Alginate chains, a BCA (bicinchoninic acid) assay was performed according to the manufacturer's protocol to measure the protein content of Alginate-P1 solutions compared to a BSA (bovine serum albumin) standard (Figure S1, Supporting Information).The C7 protein was synthesized recombinantly as previously reported.[13]

Hydrogel Preparation: The hydrogel was prepared using a 10% by weight solution of the C7 polymer mixed with a 2% by weight solution of Alginate-P1. The two components were mixed in a 1:1 ratio using a pipette. For cell encapsulation, cells were first mixed with the C7 component before being mixed with Alginate-P1 for encapsulation.

Rheological Characterization: Rheological properties were measured using a 25 mm diameter cone plate on a stress-controlled rheometer (AR-G2, TA Instrument, New Castle, DE). Components were mixed immediately before loading onto the rheometer, and a solvent trap was used to prevent dehydration of the gels. Strain sweep measurements were taken spanning 0.001%–5% strain. For shear-thinning and self-healing analysis, alternating 1 min periods of constant, linear shear was applied at rates of 0.1 and 10 s^{-1}.

Diffusivity Measurements: Diffusivity measurements were made using Fluroescence Recovery After Photobleaching (FRAP), where gels were saturated with fluorescently labeled dextrans of different sizes. Using a Leica TCS SP5 confocal microscope, an image was taken of the saturated gel at low light intensity, followed by a brief exposure to intense laser excitation, causing a 100 µm × 100 µm region of the gel to photobleach. A series of images were taken every 1.3 s for 1 min to track the recovery of dextran fluorescence. Diffusivity values were estimated using the method described by Jönsson et al.[26]

Cell Culture: Both NIH 3T3 cells and hASCs were cultured using media composed of high-glucose DMEM with L-glutamine, modified with 10% FBS (fetal bovine serum), and 1% penicillin/streptomycin. NIH 3T3 cells were purchased from Sigma-Aldrich. hASCs were isolated from deidentified human lipoaspirate from the flank and thigh regions by suction assisted liposuction. All tissue donors responded to an Informed Consent approved by the Stanford Institutional Review Board.

Printing: Printing was performed using a BioBots (Philadelphia, PA, USA) 3D bioprinter. Encapsulated cells were loaded into the cartridge of a 10 mL syringe fitted with a 32 gauge blunt-tipped nozzle (Jensen Global, Santa Barbara, CA, USA). The cartridge was then loaded into the BioBots printer, and the bioink/cell suspension was extruded at a constant pressure of 10 psi and a print speed of 4 mm s^{-1}. The material was printed onto polyethylenimine-coated microscope slides immersed in a 10×10^{-3} M $CaCl_2$ bath and allowed to cure for 10 min before moving the printed structure into cell culture medium.

Cell Settling Assay: Cells were prelabeled with Cell Vybrant DiO tracker (Thermo Fisher Scientific, Waltham, MA, USA) according to manufacturer's protocol prior to encapsulation at a concentration of 10 000 cells μL^{-1} with a total volume of 100 µL. The encapsulated cells were then placed into a plastic cuvette (Chamber volume: 70–550 µL; window dimensions: height = 3.5 mm, width = 2 mm, depth = 10 mm). The cuvette was partially sealed using styrofoam and placed in an incubator at 37 °C, 100% relative humidity, and 5% CO_2 for 1 h. Immediately after removing from the incubator, the sample was gently rotated 90° to enable confocal microscopy imaging along the entire height of the chamber.

Statistical Analysis: All data are presented as mean ± standard deviation. Statistical comparisons were performed using Student's t-test. Values were considered to be significantly different when the p value was <0.05.

Supporting Information

Supporting Information is available from the Wiley Online Library or from the author.

Acknowledgements

The authors acknowledge funding support from the National Science Foundation (DMR 1508006), the National Institutes of Health (R21 EB018407, U19 AI116484), Stanford Bio-X (IIP-7-75), Stanford Bio-X Bowes Fellowship (KD), and Stanford Bio-X Summer Undergraduate Research Program (KKL). The authors thank Prof. Michael Longaker and Dr. Elizabeth Zielins (Stanford Medical School) for help isolating hASCs, Shamik Mascharak for MATLAB script development for image processing, Prof. Kara Spiller and Prof. Wei Sun (Drexel University) for helpful discussions and bioprinter access, and Biobots, Inc. and the BioBots beta-testers community for helpful discussions.

Received: June 16, 2016
Published online:

[1] J. Malda, J. Visser, F. Melchels, T. Jungst, W. Hennink, W. Dhert, J. Groll, D. Hutmacher, *Adv. Mater.* **2013**, *25*, 5011.
[2] S. V. Murphy, A. Atala, *Nat. Biotechnol.* **2014**, *32*, 773.
[3] W. Lee, J. Pinckney, V. Lee, L. Jonh-Hwan, K. Fischer, S. Polio, J.-K. Park, *NeuroReport* **2009**, *20*, 798.
[4] S. Tasoglu, U. Demirci, *Trends Biotechnol.* **2013**, *31*, 10.
[5] W. C. Wilson, T. Boland, *Anat. Rec. A Discov. Mol. Cell Evol.* **2003**, *272A*, 491.
[6] a) M. W. Tibbitt, K. S. Anseth, *Biotechnol. Bioeng.* **2009**, *103*, 655; b) P. Bajaj, R. M. Schweller, A. Khademhosseini, J. L. West, R. Bashir, *Annu. Rev. Biomed. Eng.* **2014**, *16*, 247; c) M. Guvendiren, J. A. Burdick, *Curr. Opin. Biotechnol.* **2013**, *24*, 841.
[7] C. J. Ferris, K. J. Gilmore, S. Beirne, D. McCallum, G. G. Wallace, *Biomater. Sci.* **2013**, *1*, 224.
[8] M. E. Pepper, V. Seshadri, T. C. Burg, K. J. L. Burg, R. R. Groff, *Biofabrication* **2012**, *4*, 011001.
[9] Z. Wei, M. Xuanyi, G. Maling, M. DEqing, K. Zhang, S. Chen, *Curr. Opin. Biotechnol.* **2016**, *40*, 103.
[10] B. A. Aguado, W. Mulyasasmita, J. Su, K. J. Lampe, S. C. Heilshorn, *Tissue Eng., Part A* **2012**, *18*, 806.
[11] a) A. Skardal, J. Zhang, L. McCoard, X. Xu, S. Oottamasatien, G. D. Prestwich, *Tissue Eng., Part A* **2010**, *16*, 2675; b) A. Skardal, J. Zhang, G. D. Prestwich, *Biomaterials* **2010**, *24*, 6173.
[12] A. L. Rutz, K. E. Hyland, A. E. Jakus, W. R. Burghardt, R. N. Shah, *Adv. Mater.* **2015**, *27*, 1607.
[13] C. T. Wong Po Foo, J. S. Lee, W. Mulyasasmita, A. Parisi-Amon, S. C. Heilshorn, *Proc. Natl. Acad. Sci. USA* **2009**, *106*, 22067.
[14] W. Mulyasasmita, L. Cai, R. E. Dewi, A. Jha, S. D. Ullmann, R. H. Luong, N. F. Huang, S. C. Heilshorn, *J. Controlled Release* **2014**, *191*, 71.
[15] a) A. Parisi-Amon, W. Mulyasasmita, C. Chung, S. C. Heilshorn, *Adv. Healthcare Mater.* **2013**, *2*, 428; b) L. Cai, R. E. Dewi, S. C. Heilshorn, *Adv. Funct. Mater.* **2015**, *25*, 1344.
[16] Z. Wu, S. Xin, Y. Xi, B. Kong, W. Sun, S. Mi, *Nat. Sci. Rep.* **2016**, *6*, 24474.
[17] W. Mulyasasmita, J. S. Lee, S. C. Heilshorn, *Biomacromolecules* **2011**, *12*, 3406.
[18] K. Y. Lee, D. J. Mooney, *Prog. Polym. Sci.* **2012**, *37*, 106.
[19] S. Khalil, W. Sun, *J. Biomech. Eng.* **2009**, *13*, 111002.
[20] S. Wüst, R. Muller, S. Hofmann, *J. Funct. Biomater.* **2011**, *2*, 119.
[21] J. S. Miller, *PLoS Biol.* **2014**, *12*, e1001882.
[22] D. B. Kolesky, R. L. Truby, A. S. Gladman, T. A. Busbee, K. A. Homan, J. A. Lewis, *Adv. Mater.* **2014**, *26*, 3124.
[23] T. Wong, J. A. McGrath, H. Navsaria, *Br. J. Dermatol.* **2007**, *156*, 1149.
[24] S. Heydarkhan-Hagvall, K. Schenke-Layland, J. Q. Yang, S. Heydarkhan, Y. Xu, P. A. Zuk, W. R. MacLellan, R. E. Beygui, *Cells Tissues Organs* **2008**, *187*, 263.
[25] L. Flynn, K. A. Woodhouse, *Organogenesis* **2008**, *4*, 228.
[26] O. Jonsson, M. Jonsson, J. Tegenfeldt, F. Hook, *Biophys. J.* **2008**, *95*, 5334.